

Drift waves enstrophy, zonal flow, and nonlinear evolution of the modulational instability

Cite as: Phys. Plasmas **28**, 010702 (2021); <https://doi.org/10.1063/5.0031301>

Submitted: 29 September 2020 . Accepted: 16 December 2020 . Published Online: 11 January 2021

 S. I. Krasheninnikov,  A. I. Smolyakov,  Yanzeng Zhang, and  O. Chapurin



View Online



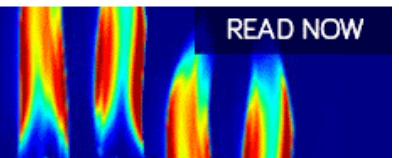
Export Citation



CrossMark

AIP Advances
Fluids and Plasmas Collection

READ NOW



Drift waves enstrophy, zonal flow, and nonlinear evolution of the modulational instability

Cite as: Phys. Plasmas **28**, 010702 (2021); doi: 10.1063/5.0031301
 Submitted: 29 September 2020 · Accepted: 16 December 2020 ·
 Published Online: 11 January 2021



S. I. Krasheninnikov,^{1,a)} A. I. Smolyakov,² Yanzeng Zhang,¹ and O. Chapurin²

AFFILIATIONS

¹Department of Mechanical and Aerospace Engineering, University of California San Diego, La Jolla, California 92093, USA

²Department of Physics and Engineering Physics, University of Saskatchewan, Saskatoon, Saskatchewan S7N 5E2, Canada

^{a)}Author to whom correspondence should be addressed: skrash@mae.ucsd.edu

ABSTRACT

The interaction of the drift wave (DW) turbulence and zonal flow (ZF) is investigated with the modified Hasegawa–Mima equation taking into account the backreaction of ZF velocity on DW turbulence. It is shown that the y-averaged enstrophy of DW turbulence and the velocity of ZF are intrinsically related. By utilizing this feature, a nonlinear stage of DW modulational instability is considered within the framework of the wave kinetic equation. It is shown that in this approximation, the nonlinear stage of the modulational instability results in the collapsing solutions, accompanied by the “wave breaking” phenomenon. Numerical simulations based on the Hasegawa–Mima equation show that for a weak DW turbulence, $\Phi = (e\bar{\phi}/T_e)(L_n/\rho_s) \ll 1$, the collapsing-like features on both ZF and y-averaged enstrophy of DW turbulence decay in time and then re-emerge again at different locations. For the case of a strong DW turbulence, $\Phi > 1$, where nonlinear interactions of DW harmonics dominate, stable spatial structures of ZF and y-averaged enstrophy of DW turbulence emerge.

Published under license by AIP Publishing. <https://doi.org/10.1063/5.0031301>

It is widely accepted that the zonal flow (ZF) plays an important role in anomalous cross field plasma transport in fusion devices and the nonlinear evolution of geophysical flows.^{1–3} In general, the generation of large-scale zonal flows is viewed as a consequence of the inverse cascade in which energy tends to concentrate in the long-wavelength part of the spectrum. The inverse cascade itself is a result of the two quadratic conserved quantities usually called “energy” and “enstrophy,” which exist in two-dimensional systems such as inviscid incompressible fluid, magnetized plasmas, and rotating geophysical fluids.^{4–7} However, both energy and enstrophy are spatially “homogeneous” and, therefore, cannot show the preferential formation of ZFs. However, in Ref. 8, it was shown that for both drift wave (DW) and Rossby wave (RW) turbulence, there also exists an anisotropic approximately conserved quadratic form, later called “zonostrophy.” The (although approximate) conservation of zonostrophy shows the preferential transfer of DW/RW energy into ZFs (see Ref. 3 and references therein).

The modulational instability of both DW and RW turbulence has long been studied,^{9,10} as a specific mechanism for the generation of ZFs. Despite a long history, the nonlinear coupling and interplay between dynamics of DW and large scale ZF (in particular, with Hasegawa–Wakatani^{12,13}-based models) is still a hot topic of ongoing research.^{3,12–15}

In this Letter, we consider the coupled DW and ZF dynamics using the modified Hasegawa–Mima equation.¹⁶ We show that the enstrophy of DW turbulence¹⁶ and ZF are directly related to each other and derive the local relation between the amplitude of the zonal flow and intensity of the quadratic enstrophy integral. This newly derived relation allows us to extend the analysis of modulational instability into the nonlinear regimes taking into account the impact of finite-amplitude ZF.¹⁶ We also show the results of numerical simulations confirming our analytical results for weak turbulence regimes and extending them into the strong turbulence case.

We consider a standard slab plasma model, with cold ions and constant uniform electron temperature, T_e , a uniform magnetic field $\vec{B} = \vec{e}_z B$, and inhomogeneous background plasma density $n_0(x)$. Coupled dynamics of ZF and drift waves is described by the modified Hasegawa–Mima equation and the equation for the evolution of the ZF in standard form (e.g., see Ref. 10),

$$\frac{\partial \hat{F}(\phi)}{\partial t} + D_B \nabla \cdot (\vec{V}_{E \times B} \hat{F}(\phi)) = -\nabla \cdot (\vec{V}_* \tilde{\phi}), \quad (1)$$

$$\frac{\partial V_0}{\partial t} \equiv -D_B \frac{\partial (\nabla \bar{\phi} \times \vec{e}_z)}{\partial t} = -D_B^2 \frac{\partial}{\partial x} \langle \tilde{V}_x \tilde{V}_y \rangle = D_B^2 \frac{\partial}{\partial x} \left\langle \frac{\partial \tilde{\phi}}{\partial x} \frac{\partial \tilde{\phi}}{\partial y} \right\rangle. \quad (2)$$

Here, $\phi = e\varphi/T_e \equiv \bar{\phi} + \tilde{\phi}$ is the normalized electrostatic potential describing both ZF, $\bar{\phi}(x, t)$, and DW turbulence, $\tilde{\phi}(x, y, t)$,

$$\hat{F}(\phi) \equiv \tilde{\phi} - \rho_s^2 \nabla^2 \phi, \quad \vec{V}_{E \times B} = -\nabla \phi \times \vec{e}_z, \quad (3)$$

where the operator $\langle \dots \rangle$ means the averaging over the y -coordinate so that the ZF part is defined as $\bar{\phi}(x, t) = \langle \phi(x, y, t) \rangle$ and DW components as $\tilde{\phi} = \phi - \bar{\phi}$. The other notations are $D_B = cT_e/eB$ and $\vec{V}_* = \vec{e}_y C_s \rho_s / L_n$, where $L_n^{-1} = -d \ln(n_0) / dx = \text{const.} > 0$, $C_s = \sqrt{T_e / M}$, with M being the ion mass, and $\rho_s = C_s / \Omega_{Bi}$, with Ω_{Bi} being the ion cyclotron frequency, which, depending in the sign of B , can be both positive and negative.

It is convenient to re-cast Eq. (1) in fully dimensionless form by using the dimensionless variables $\Phi \equiv \bar{\Phi} + \tilde{\Phi} = \phi(L_n / \rho_s)$, $\xi = \bar{r} / \rho_s$, and $\tau = t(V_* / \rho_s)$,

$$\begin{aligned} \frac{\partial}{\partial \tau} \left(\tilde{\Phi} - \nabla_{\xi}^2 \tilde{\Phi} \right) + \nabla_{\xi} \cdot \left\{ \left(\vec{e}_z \times \nabla_{\xi} \tilde{\Phi} \right) \left(\tilde{\Phi} - \nabla_{\xi}^2 \tilde{\Phi} \right) \right\} \\ = -\nabla_{\xi} \cdot \left(\vec{e}_y \tilde{\Phi} \right). \end{aligned} \quad (4)$$

From Eq. (4), one can easily see that for the characteristic wave-numbers $k\rho_s \sim 1$, or, in dimensionless form $\nabla_{\xi} \sim 1$, the nonlinear term on the left side dominates for $|\Phi| \approx 1$. In this limit, Eq. (4) will be used below for numerical simulations. For analytical considerations in the weak turbulence regime, $|\Phi| < 1$, we will use Eq. (1) to emphasize the physical parameters that define the applicability region.

It is known that Eq. (1) in the absence of ZF, $V_0(x, t) = 0$, conserves two quadratic (over $\tilde{\phi}$) forms: the effective energy, E , and enstrophy, J .¹⁰ For the case where $V_0(x, t) \neq 0$, it is easy to show that Eq. (1) conserves energy and enstrophy, defined as $E(\phi) = \tilde{\phi}^2 + \rho_s^2 (\nabla \phi)^2$ and $J(\phi) = [\hat{F}(\phi)]^2$, for any spatiotemporal variation of $V_0(x, t)$.

For our further analysis of the nonlinear stage of the modulational instability, it is useful to introduce $\hat{J}(x, t) = \langle J(\phi) \rangle$. Then, from Eq. (1), we find the following equation describing the evolution of $\hat{J}(x, t)$:

$$\frac{\partial \hat{J}}{\partial t} + \frac{\partial \Gamma_{\hat{J}}}{\partial x} = 2V_* \rho_s^2 \frac{\partial}{\partial x} \left\langle \frac{\partial \tilde{\phi}}{\partial x} \frac{\partial \tilde{\phi}}{\partial y} \right\rangle, \quad (5)$$

where

$$\Gamma_{\hat{J}} = -D_B \left\langle \frac{\partial \tilde{\phi}}{\partial y} [\hat{F}(\phi)]^2 \right\rangle \quad (6)$$

plays the role of the x -component of a nonlinear flux of the enstrophy averaged over the y -coordinate. Then, combining Eqs. (2) and (5), we find

$$\frac{\partial}{\partial t} \left(\hat{J}(x, t) - 2 \frac{MV_* V_0(x, t)}{T_e} \right) + \frac{\partial \Gamma_{\hat{J}}}{\partial x} = 0. \quad (7)$$

Thus, as we see from Eq. (7), the temporal growth of ZF and $\hat{J}(x, t)$ is related.

If we separate the contributions from zonal flow and DW turbulence in both $\hat{J}(x, t)$ and $\Gamma_{\hat{J}}(x, t)$, then Eq. (7) can be written as follows:

$$\frac{\partial \hat{J}(x, t)}{\partial t} - 2 \frac{M}{T_e} \left(V_* + \rho_s^2 \frac{\partial^2 V_0}{\partial x^2} \right) \frac{\partial V_0}{\partial t} + \frac{\partial \Gamma_{\hat{J}}}{\partial x} = 0, \quad (8)$$

where

$$\begin{aligned} \hat{J}(x, t) = \langle \hat{J}(\tilde{\phi}) \rangle \equiv \left\langle [\hat{F}(\tilde{\phi})]^2 \right\rangle, \quad \Gamma_{\hat{J}} = -D_B \left\langle \frac{\partial \tilde{\phi}}{\partial y} [\hat{F}(\tilde{\phi})]^2 \right\rangle, \\ \text{and } \hat{F}(\tilde{\phi}) \equiv \tilde{\phi} - \rho_s^2 \nabla^2 \tilde{\phi}. \end{aligned} \quad (9)$$

Equation (8) plays a crucial role in our further analysis of the nonlinear stage of the modulational instability.

To make a qualitative evaluation of coupled dynamics of DW and ZF, we will assume the spatiotemporal scale lengths of ZF, $(T, \Lambda)_{ZF}$, are much larger than those of DW turbulence, $(\omega^{-1}, \lambda)_{DW}$. Therefore, we neglect the term $\propto \partial^2 V_0 / \partial x^2$ in Eq. (8). In addition, since $\Gamma_{\hat{J}} \propto |\tilde{\phi}|^3$ and $\hat{J}(x, t) \propto |\tilde{\phi}|^2$, for the case of weak turbulence, implying that $|\tilde{\phi}| \ll 1$, $\Gamma_{\hat{J}}$ is a higher order term in comparison with $\hat{J}(x, t)$ and can be neglected. Neglect of the enstrophy flux $\Gamma_{\hat{J}} \propto |\tilde{\phi}|^3$ in Eq. (8) is consistent with the growth rate of the modulational instability $\propto |\tilde{\phi}|$ in the hydrodynamic limit.¹⁰ As a result, within these simplifications, Eq. (8) is reduced to

$$\hat{J}(x, t) - 2 \frac{MV_* V_0(x, t)}{T_e} = \hat{J}(x, t = 0) \equiv \hat{J}_0 = \text{const.}, \quad (10)$$

where we assume an initially homogeneous profile of $\hat{J}(x, t = 0)$. From Eq. (10), we see that the generation of ZF is directly related to the departure of $\hat{J}(x, t)$ from its original value. Assuming that $\lambda_{DW} \sim \rho_s$ and estimating the amplitude of ZF from Eq. (10), we find $V_0 / V_* \sim \tilde{\phi}^2 (L_n / \rho_s)^2$. Therefore, the term $\propto \partial^2 V_0 / \partial x^2$ in Eq. (8) can be neglected for

$$|\tilde{\phi}| \ll \Lambda_{ZF} / L_n < 1 \rightarrow |\tilde{\Phi}| \ll \Lambda_{ZF} / \rho_s. \quad (11)$$

For $\Lambda_{ZF} \sim \rho_s$, we find that relation (10) holds for $|\tilde{\Phi}| \ll 1$, whereas for the higher amplitude of DW turbulence, all terms in Eq. (8) should be retained.

We notice that for the case where $(T, \Lambda)_{ZF}$ are much larger than $(\omega^{-1}, \lambda)_{DW}$, the enstrophy $\hat{J}(\tilde{\phi})$ becomes an adiabatic invariant,^{17,18} and to describe the interactions of DW with ZF, we can use the “kinetic” equation for the spectral density of $\hat{J}(\tilde{\phi})$ (e.g., see Ref. 10). Although the wave kinetic approximation is valid only for limited range DW and ZF parameters, it gives further insights into the nonlinear features of DW and ZF interaction.

The kinetic equation for the spectral density of DW enstrophy has the form¹¹

$$\frac{\partial \tilde{J}_{\vec{k}}}{\partial t} + \nabla \cdot \left(\vec{V}_{\vec{k}} \tilde{J}_{\vec{k}} \right) + \nabla_{\vec{k}} \cdot \left(\vec{W}_{\vec{k}} \tilde{J}_{\vec{k}} \right) = 0, \quad (12)$$

where $\tilde{J}_{\vec{k}}(\vec{r}, t) = (1 + \rho_s^2 k^2)^2 I_{\vec{k}}(\vec{r}, t)$, $I_{\vec{k}}(\vec{r}, t)$ is the normalized DW turbulence spectral function written in Wigner’s form $I_{\vec{k}}(\vec{r}, t) = \int d\vec{q} \tilde{\phi}_{-\vec{k}+\vec{q}/2} \tilde{\phi}_{\vec{k}+\vec{q}/2} \exp(i\vec{q} \cdot \vec{r})$, and $\tilde{\phi}_{\vec{k}}$ is the Fourier component of normalized electrostatic potential. In what follows, we assume that $I_{\vec{k}}(\vec{r}, t)$ only depends on the x -coordinate.

To find the expressions for the velocities of the wave packet in real, $\vec{V}_{\vec{k}}$, and k -space, $\vec{W}_{\vec{k}}$, we use the following expression for the frequency of DW in the presence of ZF:

$$\omega = \frac{V_* k_y}{1 + \rho_s^2 k^2} + V_0(x, t) k_y. \quad (13)$$

Then, we find the x-component of the “quasi-particle” velocity in real space, dx/dt (group velocity of the wave packet V_{gr}),

$$\frac{dx}{dt} \equiv (\vec{V}_{\vec{k}})_x \equiv V_{gr} = \frac{\partial\omega}{\partial k_x} = -2V_* \frac{k_x k_y}{(1 + \rho_s^2 k^2)^2}, \quad (14)$$

and k-space,

$$\frac{dk_x}{dt} = (\vec{W}_{\vec{k}})_x = -\frac{\partial\omega}{\partial x} = -\frac{\partial V_0}{\partial x} k_y. \quad (15)$$

Equation (2) for $V_0(x, t)$, expressed in terms of $I_{\vec{k}}(\vec{r}, t)$, has the form

$$\frac{\partial V_0}{\partial t} = C_s^2 \rho_s^2 \frac{\partial}{\partial x} \left(\int k_x k_y I_{\vec{k}}(\vec{r}, t) d\vec{k} \right). \quad (16)$$

Then, integrating kinetic equation (12) over \vec{k} and using expression (14), we arrive to Eq. (10) written in terms of spectral density of the enstrophy, $\hat{J}(x, t) = \int \tilde{J}_{\vec{k}} d\vec{k}$.

Equation (10), which is a “subset” of exact Eq. (8), is valid for the case of relatively weak DW turbulence defined by inequality (11). In the weak turbulence regime, the magnitude of ZF is smaller than V_* , which allows us neglect the term $\propto \partial^2 V_0 / \partial x^2$ in both Eq. (8) and in the derivation of kinetic equation (12). In this regime, the effective “self-collisions” of the small-scale DW fluctuations (e.g., see Ref. 5), which correspond to the enstrophy flux term in Eq. (8), are the higher order terms with respect to $|\hat{\phi}|$ and also can be neglected.

Let us take $V_* > 0$ and consider the wave packets having the wave number $\vec{k} = \vec{k}_0$ and the initially homogeneous intensity profile $I_{\vec{k}_0}(x)$. Assume now that $I_{\vec{k}_0}(x)$ and $\hat{J}(x)$ experience some spatial perturbations. In the first order, if we ignore an impact of ZF on the dynamics of DW, the spatial structures of $\hat{J}(x)$ and $V_0(x)$ will propagate into the positive direction along x with group velocity $V_{gr}(k_0)$ (we assume $k_x k_y < 0$). In the next order, when the ZF effects on the wave-packet propagation are included, one obtains the linear stage of the modulational instability, which can be interpreted based on Eq. (10). From Eq. (15), one can see that the spatial variation of the magnitude of ZF velocity causes the variation of k_x and, therefore, the group velocity $(V_{\vec{k}})_x$. In other words, the wave packet will experience the acceleration $a_{gr} \equiv d^2x/dt^2$. From Eqs. (14) and (15), we find

$$a_{gr} = 2V_* \frac{\rho_s^2 k_y^2}{(1 + \rho_s^2 k^2)^3} \left[1 + \rho_s^2 (k_y^2 - 3k_x^2) \right] \frac{\partial V_0}{\partial x}. \quad (17)$$

One can see from (17) that for the wave packet with the localized perturbation of $V_0(x)$ and provided that

$$1 + \rho_s^2 (k_y^2 - 3k_x^2) > 0, \quad (18)$$

the region with $\partial V_0(x)/\partial x < 0$ is decelerated, while the region with $\partial V_0(x)/\partial x > 0$ is accelerated. This leads to shrinking of the wave packet perturbation. Since $\hat{J}(x)$ is constant on the characteristic equations (14) and (15), shrinking of the wave packet leads to the enhancement of the perturbation of $\hat{J}(x)$ and, according to Eq. (10), to the enhancement of the ZF perturbation $V_0(x)$. Alternatively, the increase in the perturbation $\hat{J}(x)$ due to the wave packet shrinking can be seen as a result of the conservation of the total integral $\int \hat{J}(x) dx$ [which follows from Eq. (12)]. As a result, the $\hat{J}(x)$ amplitude (hence the

amplitude of $V_0(x)$) increases when the wave packet becomes narrower. This picture describes the modulational instability in the DW and ZF system¹⁰ and inequality (18) ensures such instability in a hydrodynamic limit.

Equation (10) also allows us to describe a nonlinear stage of the modulational instability of the initially homogeneous profile of the enstrophy for the wave packet with the wave number $\vec{k} = \vec{k}_0$. To simplify the algebra, we will consider the case $\rho_s^2 k^2 \ll 1$ so that inequality (18), predicting modulational instability, holds. Then, introducing the dimensionless variables $U(x, t) = V_{gr}(x, t)/\bar{V}_{gr} - 1$, and $S(x, \tau) = (\hat{J}(x, \tau)/4)(L_n/\rho_s)^2 \rho_s^{-2} (k_0)_x^{-2}$, Eqs. (12) and (15) can be written as

$$\frac{\partial S}{\partial \tau} + \frac{\partial}{\partial x}(US) = 0, \quad (19)$$

$$\frac{\partial U}{\partial \tau} + U \frac{\partial U}{\partial x} = \frac{\partial S}{\partial x}, \quad (20a)$$

respectively, where $\tau = \bar{V}_{gr} t$ and $\bar{V}_{gr} = -2V_* \rho_s^2 (k_0)_x (k_0)_y$. The evolution of $U(x, t) \sim V_{gr}(x, t)$ in Eq. (20a) is related to the evolution of the wavevector k_x in Eq. (15) and the relation $\bar{V}_{gr} \propto -2V_* \rho_s^2 k_x k_y$ from Eq. (14). We have also used the relation between $\hat{J}(x, t)$ and $V_0(x, t)$ from Eq. (10) and transformed to the frame moving with velocity \bar{V}_{gr} .

Equations (19) and (20a) belong to the wide class of the so-called “quasi-Chaplygin” media having negative compressibility and, therefore, intrinsically unstable.¹⁹ For the first time, an example of the gas with negative compressibility was considered in 1896 by Chaplygin.²⁰ For such gas, the S variable in (19) is related to the density, and the momentum equation for the gas velocity U takes the form of Eq. (20a) where gas pressure was assumed with $\gamma = -1$ adiabat, i.e., the following relation between the pressure P and density $\rho: P = P_0 \rho_0 / \rho$. Many instabilities in plasmas and fluids, in the nonlinear regime (typically in the long wavelength limit), can be reduced to the nonlinear quasi-Chaplygin gas equations in the form of Eq. (19) and more general equation in the form

$$\frac{\partial U}{\partial \tau} + U \frac{\partial U}{\partial x} = \frac{1}{p} \frac{\partial S^p}{\partial x}, \quad (20b)$$

with different values of the parameter p. Examples of such instabilities, characterized by different values of p, can be found in Ref. 19 and references therein.

In Ref. 19, it was shown that using the hodograph transformation, one can transform nonlinear equations (19) and (20b) to the linear equations for the functions $x = X(U, S^{p/2})$ and $\tau = T(U, S^{p/2})$. In Ref. 19, different solutions for quasi-Chaplygin equations, corresponding to $U(x, \tau \rightarrow -\infty) = 0$ and $S(x, \tau \rightarrow -\infty) = S_0$ (in our case, $S_0 = (\hat{J}_0/4)(L_n/\rho_s)^2 \rho_s^{-2} (k_0)_x^{-2}$) were obtained corresponding, in particular, to the soliton-like and periodic structures in the x-direction. The implicit expressions for such solutions for $U(x, \tau)$ and $S(x, \tau)$ can be found in Ref. 19. An example of such solutions describing nonlinear development of the modulational instability is shown in Fig. 5 from Ref. 20. In all cases considered in Ref. 19, the evolution of $S(x, t) \propto \hat{J}(x, t)$ at $t = t_{crit}$ ends up with the appearance of singularities at some points in space, $x = x_0$, where $S(x_0) = 0$, whereas $|dS/dx|_{x=x_0} = \infty$ so that strictly speaking no physically meaningful solution exist at $t > t_{crit}$. We note that the formation of the singularities in the coupled ZF and RW evolution was also reported in Ref. 4.

We should note, however, that unlike quasi-Chaplygin solutions considered in Ref. 19, in our case $U(x, \tau)$ cannot fall below -1 since it corresponds to the “reflection” of the wave packet and after that we have to deal with a multi-valued flow, which cannot be described anymore with Eqs. (19) and (20a). As a result, the applicability of the solutions of Eqs. (19) and (20a) is limited by the inequality

$$U(x, \tau) \geq -1. \tag{21}$$

The wave packet approximation for DW evolution cannot be applied for the case of sharp gradients of $\hat{J}(x, t)$. Therefore, the solutions found in Ref. 19 only can be used for $t < t_{crit}$. On the other hand, outside of the points $x = x_0$, our wave packet approximation is still valid and, therefore, the nonlinear stage of the modulational instability accompanied by the increase in the amplitudes and sharpening of spatial profiles of $\hat{J}(x, t)$ and $V_0(x, t)$ can still be described by Eqs. (19) and (20a).

So far, we consider the nonlinear evolution of the wave packets having initially the same group velocity, which implies that $k_x(0)$ is either positive or negative. However, for example, the growth rate of resistive drift waves does not depend on the sign of k_x and, therefore, it is interesting to consider the nonlinear stage of the modulational instability where the wave packets of the same intensity propagate into opposite directions. In this case, considering $\rho_s^2 k^2 \ll 1$, we arrive at the following system of equations describing the nonlinear evolution of the modulational instability:

$$\frac{\partial S_{(\pm)}}{\partial \tau} + \frac{\partial}{\partial x}(U_{(\pm)} S_{(\pm)}) = 0, \tag{22}$$

$$\frac{\partial U_{(\pm)}}{\partial \tau} + U_{(\pm)} \frac{\partial U_{(\pm)}}{\partial x} = \frac{\partial(S_{(+)} + S_{(-)})}{\partial x}, \tag{23}$$

where $\tau = |\bar{V}_{gr}|t$, $U_{(\pm)}(x, \tau) = V_{gr}^{(\pm)}(x, \tau)/|\bar{V}_{gr}|$ are the normalized group velocities of the wave packets moving to $x \rightarrow \pm\infty$, $S_{(\pm)}(x, \tau) = (\hat{J}_{(\pm)}(x, \tau)/4)(L_n/\rho_s)^2 \rho_s^{-2}(k_0)_x^{-2}$ are their normalized intensities, and $|\bar{V}_{gr}| = 2|V_* \rho_s^2(k_0)_x(k_0)_y|$.

We consider the solutions of Eqs. (22) and (23) with the following initial conditions: $U_{(\pm)}(x, \tau = 0) = \pm 1$ and $S_{(\pm)}(x, \tau = 0) = S_0/2$, where S_0 is some constant. A small initial perturbation with fixed periodic boundary conditions was added to initiate the evolution. The linear stability analysis of two counter-propagating monochromatic drift waves against the modulational instability was considered in Ref. 21. The results found in Ref. 21 can be easily obtained from the linearized system of equations (21) and (22). However, actually the results of Ref. 16 are only valid for the case corresponding to $S_0 < 1$, when one can neglect a broadening, $\Delta(|\Omega/q|) \approx \sqrt{S_0}$, of the resonance $|\Omega/q| = 1$, where Ω and q are the normalized frequency and the wave number of the modulational instability, respectively. In order to separate two wave packets, the same restriction, $S_0 < 1$, holds for the applicability of Eqs. (22) and (23).

For the case of two wave packets propagating in opposite directions, the nonlinear stage of the modulational instability, which causes

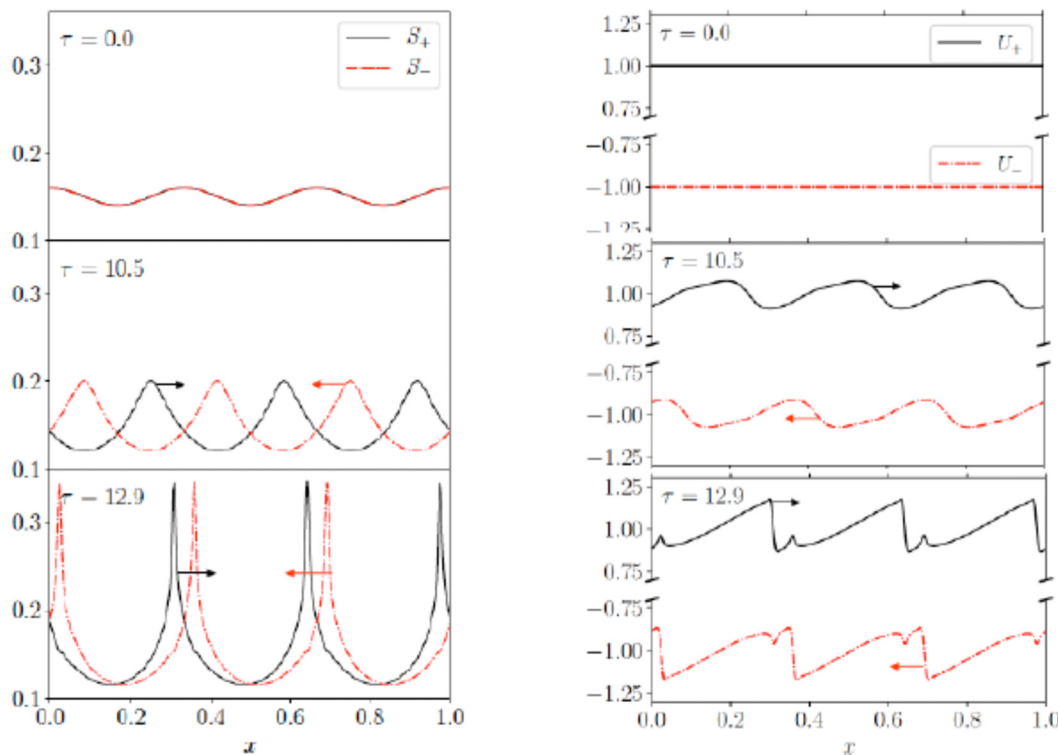


FIG. 1. The evolution of $S_{(\pm)}(x, \tau)$ (left) and $U_{(\pm)}(x, \tau)$ (right), from numerical solution of Eqs. (22) and (23), shows the growth of perturbations due to the modulational instability and wave breaking. The arrows show the directions of the propagation for $S_{(\pm)}(x, \tau)$ and $U_{(\pm)}(x, \tau)$.

the variation of the group velocities, is accompanied by the wave breaking phenomenon. It is well known that the wave breaking results in a local spatial increase in the effective “density” (in our case, $S_{(\pm)}(x, \tau)$), which, in some sense, facilitates the effect of the modulational instability.

The results of numerical solution of Eqs. (22) and (23) with periodic boundary conditions, illustrating the effects of the growth of the modulational instability and the wave breaking, are shown in Fig. 1.

These results again show the “collapsing”-spatial profiles of $S_{(\pm)}(x, \tau)$, which limits the applicability of our wave packet based approximation, only valid for $k_x \Delta_{(\pm)} < 1$, where $\Delta_{(\pm)}$ are the characteristic widths of $S_{(\pm)}(x, \tau)$.

To verify our analytical and semi-analytical considerations and go beyond the weak DW turbulence approximation, we perform additional studies based on numerical integration of Eq. (4) with a pseudo-spectral Fourier code. The computation domain in our simulation was a square box with the size $L_x = L_y = 20\pi\rho_s$ so that the lowest wavenumber is $\rho_s k_{min} = 0.1$ and the number of the modes is 528^2 . We use doubly periodic boundary conditions and the fourth-order Runge–Kutta method as the time integration algorithm. For the simulations, we use the dimensionless variables: $\Phi = \phi(L_n/\rho_s)$, $\xi = \vec{r}/\rho_s$, and $\tau = t(V_*/\rho_s)$. The time step of the integration was $\Delta\tau = 5 \times 10^{-3}$. The seed for DW turbulence for our numerical solution of Eq. (4) was obtained from the simulation of fully

turbulent stage of the Hasegawa–Wakatani model with no zonal components.

In Fig. 2, one can see the time evolution of normalized $\hat{J}(x, t)$, $V_0(x, t)$, and the $\hat{J}(x, t) - 2MV_*V_0(x, t)/T_e$ quantity found from numerical simulations for different amplitudes of initial dimensionless DW turbulence: $|\tilde{\Phi}| \approx 10^{-2}$, $|\tilde{\Phi}| \approx 0.3$, and $|\tilde{\Phi}| \approx 3$. Such magnitudes of initial dimensionless DW turbulence correspond, according to Eq. (11), to the transition from a weak to a strong DW turbulence where a nonlinear term in Eq. (4) starts to dominate. The relative deviations of total energy and enstrophy in these simulations were, respectively, within 10^{-8} and 10^{-5} for $|\tilde{\Phi}| \approx 10^{-2}$, 3×10^{-6} and 10^{-4} for $|\tilde{\Phi}| \approx 0.3$, and 6×10^{-6} and 2×10^{-4} for $|\tilde{\Phi}| \approx 3$.

From Fig. 2, one can see that in accordance with our qualitative physical picture, for the case of a weak DW turbulence, $|\tilde{\Phi}| \approx 10^{-2}$ and $|\tilde{\Phi}| \approx 0.3$, the difference $\hat{J}(x, t) - 2MV_*V_0(x, t)/T_e$ is conserved rather well over entire simulation time. However, for the $|\tilde{\Phi}| \approx 0.3$ case, there is some initial phase of adjustment of ZF and $\hat{J}(x, t)$. The spatiotemporal variation of $\hat{J}(x, t)$ and $V_0(x, t)$ is rather coherent. The results of the simulations show the forming of the “peaks” of spatial distributions of $\hat{J}(x, t)$ and $V_0(x, t)$, which then decay later. Such events happen intermittently at different locations along the x-coordinate.

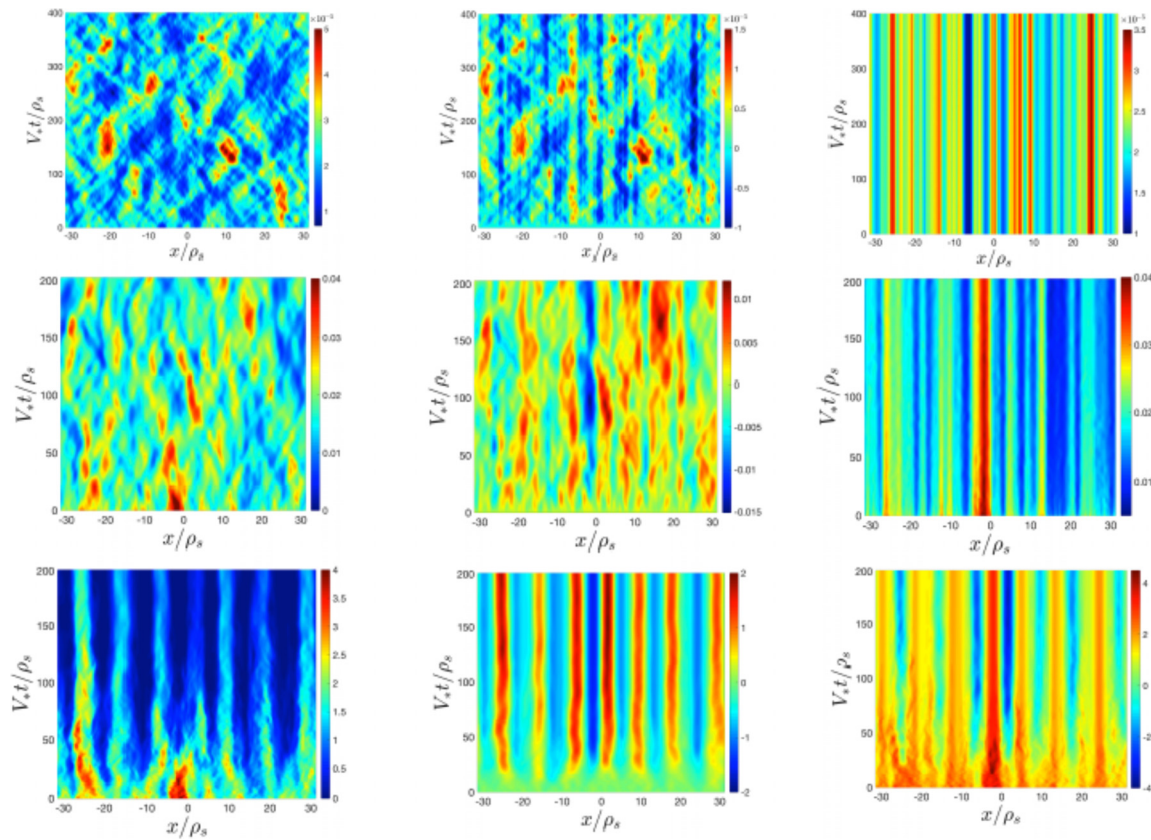


FIG. 2. Time evolution of normalized DW enstrophy $\hat{J}(x, t)$ (left), the velocity of the zonal flow velocity $V_0(x, t)$ (center), and the difference $\hat{J}(x, t) - 2MV_*V_0(x, t)/T_e$ (right) for different initial amplitudes of DW turbulence $|\tilde{\Phi}| \approx 10^{-2}$ (top panel), $|\tilde{\Phi}| \approx 0.3$ (central panel), and $|\tilde{\Phi}| \approx 3$ (bottom panel).

For the case of a strong DW turbulence, $|\tilde{\Phi}| \approx 3$, where nonlinear interactions of DW harmonics dominate, in the beginning of the simulation, there is some adjustment between $\hat{J}(x, t)$ and $V_0(x, t)$ after which a rather stable ZF spatial structure, which entrains the DW turbulence, is formed and the difference $\hat{J}(x, t) - 2MV_*V_0(x, t)/T_e$ remains largely constant after that.

In conclusion, we have considered the interaction of the DW turbulence and ZF within the modified Hasegawa–Mima equation¹⁰ taking into account nonlinear feedback effects from ZF.⁵ One of our principal results is a finding that γ -averaged enstrophy of DW turbulence, $\hat{J}(x, t)$, and the velocity of ZF, $V_0(x, t)$, are related [see Eq. (8)]. This relation shows that the generation of ZF by DW turbulence is accompanied by the local growth of the averaged enstrophy, $\hat{J}(x, t)$, which is redistributed in space. Recall that the enstrophy is conserved globally. By utilizing the relation between $\hat{J}(x, t)$ and $V_0(x, t)$, we have considered the nonlinear stage of DW modulational instability in the framework of wave packet approximation relevant for a weak DW turbulence satisfying the inequalities (11). We show that the nonlinear evolution of DW and ZF proceeds to the formation of narrow spatially localized structures in $\hat{J}(x, t)$ and $V_0(x, t)$ (collapsing solutions). This analytical result is confirmed by our numerical simulations of the extended Hasegawa–Mima equation in the weak turbulence limit.

Our simulations, which go beyond the wave packet approximation, also show that collapse of the spatial profiles of $\hat{J}(x, t)$ and $V_0(x, t)$ is terminated at some level, with the subsequent spreading in space and further re-occurrence at different spatial locations. We suggest that this is a result of the breaking down of the quasi-classical approximation (wave packet) in the collapsing stage with the narrowly localized structures so our analytical theory is no longer applicable. Our numerical simulations also show that for strong DW turbulence, $|\tilde{\Phi}| \gtrsim 1$, the nonlinear interactions of DW harmonics result in the generation of standing DW in the vicinity of the peaks of $\hat{J}(x, t)$ and $V_0(x, t)$, which prevents their decay. These results provide the information of the nonlinear saturated states (amplitude and spatial length scales) of the zonal flow from the nonlinear evolution of the developed turbulence. The next steps would be to investigate these solutions in the unstable regimes with continuing energy input from the instabilities, which is left for future studies.

This work was supported by the U.S. Department of Energy, Office of Science, Office of Fusion Energy Sciences under Award No. DE-FG02-04ER54739 at UCSD, and NSERC Canada.

DATA AVAILABILITY

The data that support the findings of this study are available from the corresponding author upon reasonable request.

REFERENCES

- ¹P. H. Diamond, S. Itoh, K. Itoh, and T. Hahm, “Zonal flows in plasma: A review,” *Plasma Phys. Controlled Fusion* **47**, R35 (2005).
- ²A. Fujisawa, “A review of zonal flow experiments,” *Nucl. Fusion* **49**, 013001 (2009).
- ³C. Connaughton, S. Nazarenko, and B. Quinn, “Rossby and drift wave turbulence and zonal flows: The Charney–Hasegawa–Mima model and its extensions,” *Phys. Rep.* **604**, 1 (2015).
- ⁴T. D. Lee, “Difference between turbulence in a two-dimensional fluid and three-dimensional fluid,” *J. Appl. Phys.* **22**, 524 (1951).
- ⁵R. Fjørtoft, “On the changes in the spectral distribution of kinetic energy in two-dimensional, nondivergent flow,” *Tellus* **5**, 225–230 (1953).
- ⁶E. N. Lorenz, “Barotropic instability of Rossby motion,” *J. Atmos. Sci.* **29**, 258–264 (1972).
- ⁷A. Hasegawa, C. G. MacLennan, and Y. Kodama, “Nonlinear behavior and turbulence spectra of drift waves and Rossby waves,” *Phys. Fluids* **22**, 2122–2129 (1979).
- ⁸A. Balk, “A new invariant for Rossby wave systems,” *Phys. Lett. A* **155**, 20–24 (1991).
- ⁹D. Yu. Manin and S. V. Nazarenko, “Nonlinear interaction of small-scale Rossby waves with an intense large-scale zonal flow,” *Phys. Fluids* **6**, 1158 (1994).
- ¹⁰A. I. Smolyakov, P. H. Diamond, and M. Malkov, “Coherent structure phenomena in drift wave–zonal flow turbulence,” *Phys. Rev. Lett.* **84**, 491 (2000).
- ¹¹A. Hasegawa and M. Wakatani, “Plasma edge turbulence,” *Phys. Rev. Lett.* **50**, 682 (1983).
- ¹²R. Numata, R. Ball, and R. L. Dewar, “Bifurcation in electrostatic resistive drift wave turbulence,” *Phys. Plasmas* **14**, 102312 (2007).
- ¹³C.-B. Kim, “Suppression of turbulence in the drift-resistive plasma where zonal flow changes direction,” *J. Plasma Phys.* **86**, 905860315 (2020).
- ¹⁴H. Zhu, Y. Zhou, and I. Dodin, “Theory of the tertiary instability and the Dimits shift from reduced drift-wave models,” *Phys. Rev. Lett.* **124**, 055002 (2020).
- ¹⁵Y. Zhang and S. I. Krasheninnikov, “Effect of neutrals on the anomalous edge plasma transport,” *Plasma Phys. Controlled Fusion* **62**, 115018 (2020).
- ¹⁶A. Hasegawa and K. Mima, “Pseudo-three-dimensional turbulence in magnetized nonuniform plasma,” *Phys. Fluids* **21**, 87 (1978).
- ¹⁷A. I. Smolyakov and P. H. Diamond, “Generalized action invariants for drift waves–zonal flow systems,” *Phys. Plasmas* **6**, 4410 (1999).
- ¹⁸J. A. Krommes and C.-B. Kim, “Interactions of disparate scales in drift-wave turbulence,” *Phys. Rev. E* **62**, 8508 (2000).
- ¹⁹B. A. Trubnikov and S. K. Zhdanov, “Unstable quasi-gaseous media,” *Phys. Rep.* **155**, 137 (1987).
- ²⁰C. A. Чаплыгин “Избранные труды,” Москва, Наука, 1976, с. 94 [S. A. Chaplygin, *Selected Papers* (Nauka, Moscow, 1976), p. 94 (in Russian)].
- ²¹A. B. Mikhailovskii, M. S. Shirokov, A. I. Smolyakov, and V. S. Tsypin, “Two-stream-like mechanism of zonal-flow generation by Rossby waves in a shallow rotating fluid,” *JETP Lett.* **84**, 76 (2006).